Scientific Research Publishing

Materials Sciences and Applications, 2019, 10, 12-24
http://www.scirp.org/journal/msa
ISSN Online: 2153-1188
ISSN Print: 2153-117X

Ion Radiation Detection Using Implanted Ultrahigh Molecular Weight Polyethylene Structures (UHMWPE)

Maitha El-Muraikhi

Mathematic, Statistic & Physics Department, Faculty of Art & Science, Qatar University, Doha, Qatar
Email: mdmuraikhi@qu.edu.qa

How to cite this paper: El-Muraikhi, M. (2019) Ion Radiation Detection Using Implanted Ultrahigh Molecular Weight Polyethylene Structures (UHMWPE). *Materials Sciences and Applications*, **10**, 12-24.
https://doi.org/10.4236/msa.2019.101002

Received: December 1, 2018
Accepted: January 4, 2019
Published: January 7, 2019

Abstract

The effect of ion implantation, including Ar^+ ion with influences (1×10^{13} - 10^{15} ions/cm^2), on the electrical and optical properties of ultrahigh molecular weight polyethylene (UHMWPE) were investigated with particular emphasis placed on the sensor performance to be used in the field of radiation detection. The obtained results focusing on the effect of the different influences showed a significant change in the electrical conductivity, capacitance and loss tangent. The absorption spectra for UHMWPE samples were recorded and the values of the allowed direct and indirect optical energy gap $(E_{opt})^d$, $(E_{opt})^{in}$ of UHMWPE and energies of the localized states for the virgin and implanted samples were calculated. We found that the optical energy gap values decreased as the radiation dose increased. The results can be explained on the basis of the ion beam radiation-induced damage in the linear chains of UHMWPE, with cross-linking generated after implantation. The observed changes in both the optical and the electrical properties suggest that the UHMWPE film may be considered as an effective material to achieve ion-radiation detection at room temperature.

Keywords

Ultrahigh Molecular Weight Polyethylene, Ion Beam Irradiation, UV-Vis Spectroscopy, Ion Detection, Optical Band Gap, Dielectric Constant

1. Introduction

Ion implantation is a technology in which one type of external action leads to various defects in materials. The ion beam irradiation affects the polymer structure by cross-linking and degradation [1]. The bombardment of polymers by

energetic ions produces dramatic changes due to disruption of original chemical bonding [2]. This eventually results in cross-linking and chain scission, which can produce metastable layers in materials via non-equilibrium processes [3]. The interest in the irradiation of polymers with high energy ions originated from their ability to register nuclear tracks and the applications of polymers as particle detectors or as membranes, which are widely described in the literature [4] [5] [6]. Radiation damage can be measured by a number of different methods, including the solid state nuclear track detector as gamma-ray dosimeter [7]. Generally, the radiation interactions with plastic detectors causes a reduction in the average molecular weight of the latter, which subsequently produces an enhancement in the bulk due to high energy radiation as the γ-dose increases [8]. Ion beam treatment provides a unique way to modify the chemical, structural, optical, mechanical and electrical properties of the polymers by causing irreversible changes in their macromolecular structure. It can be used to change, in a controlled way, the physical properties of the films or to modify the near-surface characteristics of a bulk polymer [9]. Koizumi *et al.* [10] found that the radical yield is constant at a lower dose and decreases with increasing ion influence. Furthermore, Abdul-Kader *et al.* [11] studied the changes in the surface layer composition produced by different ion bombardment of polyethylene and isotactic polypropylene. They have observed important hydrogen release with increasing ion dose and they have correlated it with linear energy transfer (LET). Ion implantation technology has been successfully applied to the modification of polymers for improving their surface properties, such as electrical resistance, and optical properties [12] [13]. The increase in the wear resistance of UHMWPE has been achieved by ion implantation [2] [14] [15]. The irradiation effects of ion beams were studied with respect to their structural and electrical properties by Wu *et al.* [16]. It is well known that irradiation enhances the electrical conductivity in insulating polymers. This increase in conductivity was attributed to the amplifications of the conjugated structure, which indicates relatively great electron freedom. The irregularity in the polymer chains may also give rise to a hopping mechanism, which will enhance the conductivity. Moreover, the effects of radiation on dielectric properties are of particular interest to science and technology and they have many applications in modern engineering [17] [18] [19].

The extent and the type of defects depend on the nature of radiation as well as its energy and dose. As a result of irradiation, the chemical bonds are damaged and various types of radicals are created. Chen *et al.* [14] and Allen *et al.* [15] studied the effects of irradiation by various energetic ions on the physical properties of UHMWPE. The large doses of irradiation caused by the presence of oxygen and UV irradiation were found to influence the response and sensitivity of detectors [5] [20], but the data available for ultrahigh molecular weight polyethylene and the effect of ion radiation on the physical properties are not sufficient. However, there has not been detailed examination of the changes in the

electrical and optical properties due to ion irradiation on UHMWPE. Therefore, in the present work, the author reports the effects of 160 keV Ar ion irradiation on both the electrical and optical properties of UHMWPE structures at different influences. By gaining sufficient knowledge about the ion radiation, the induced effect indicates that this is suitable for use as sensitive ion beam dosimeters.

2. Experimental Techniques

2.1. Sample Preparation

The studied UHMWPE was supplied by Goodfellow Ltd. (Cambridge, UK). The processing characteristics included M_w = 120,000 g/mol, M_w/M_n = 3.4, T_m = 132˚C, T_c = 112˚C and density d = 0.95 g/cm^3. The polymer samples used were flat, rectangular wafers with a thickness of 1 mm.

Ion bombardment was carried out in a vacuum at room temperature by means of commercial blazers MPB 202 RP ion implanter at the institute of Electronic Material Technology (ITME), Poland. The beam density was maintained below 0.1 A/cm in order prevent any increases in the sample temperature. The 160 and 300 keV Argon influences ranged from 1×10^{13} to 1×10^{15} ions/cm^2, which were originally applied by Turos *et al.* [21].

2.2. Optical Measurements

The absorption spectra of the virgin and treated samples were recorded in the wavelength range of 200 - 1100 nm using a lambda 950 Perkin Elmer UV-Vis spectrometer. A perfectly flat piece of the UHMWPE thin sheet was placed vertically in the path of the sample beam, while the reference beam directly reached the detection point. Therefore, the spectral data obtained are absolute values.

2.3. Dielectric Measurements

The electrical properties of all samples were studied before and after ion implantation. The electrical contacts were made to the samples using silver paste. After this, the impedance, resistance, dielectric loss (tanδ) and capacitance measurements were carried out using a Hewlett Packard 4284A LCR meter, which was operated at 0.8 V over the frequency range of 100 Hz - 1 MHz at room temperature. The AC conductivity was calculated using the relation $\sigma(\omega) = t/\mathrm{AR}$. The dielectric constant was calculated using the relationships of $\varepsilon = C_p/C_o$, where C_p is the capacitance measured using the LCR meter; and $C_o = \varepsilon_o A/t$, where ε_o is the permittivity of vacuum and A and t are the cross-sectional area and thickness of the sample, respectively. The exposed area was 0.083 cm^2 and the measurements were performed in air.

3. Results and Discussions

3.1. Optical Properties for UHMWPE

The study of the optical absorption and particularly the absorption band edge is a useful tool for providing information about the electronic band structure, loca-

lized states, type of optical transition and optical energy gap in polymeric materials [22]. **Figure 1** shows the typical plots of the absorption spectra before and after ion implantation for UHMWPE samples with a thickness of 1 mm. From the picture, it is evident that the optical absorption spectral distribution is sensitive to the radiation influence. With an increase in the ion dose, a consequent enhancement in the intensity of the absorption was observed. Generally, the radiation interaction with plastic detectors causes a reduction in the average molecular weight of the latter. The implantation induced alteration of the polymer structure and composition changes optical properties. It is believed that the ionizing radiation causes structural defects (called color centers or oxygen vacancies in oxides), leading to their density change upon the exposure to the rays [23].

Optically transparent polymers acquire some color after implantation. The color changes to deep brown or grey with increasing ion influence, while a metallic luster appears at high influences (1×10^{15} cm^{-2}), which is fairly consistent with a previous study [1]. This phenomenon is consistent with the red shift of the absorption edge, which is shown in **Figure 1**. This is due to an increase in the average band gap in the conjugated polymer system, which causes lower energy to be received by ion bombardment. According to Planck's constant formula, $E = hc/\lambda$, as the wavelength increases, the energy required for electron transition between the localized states will be less. This results in the position of the fundamental absorption edge shifting towards larger wavelengths. This behavior can be attributed to the fact that the degradation of sample starts at a dose

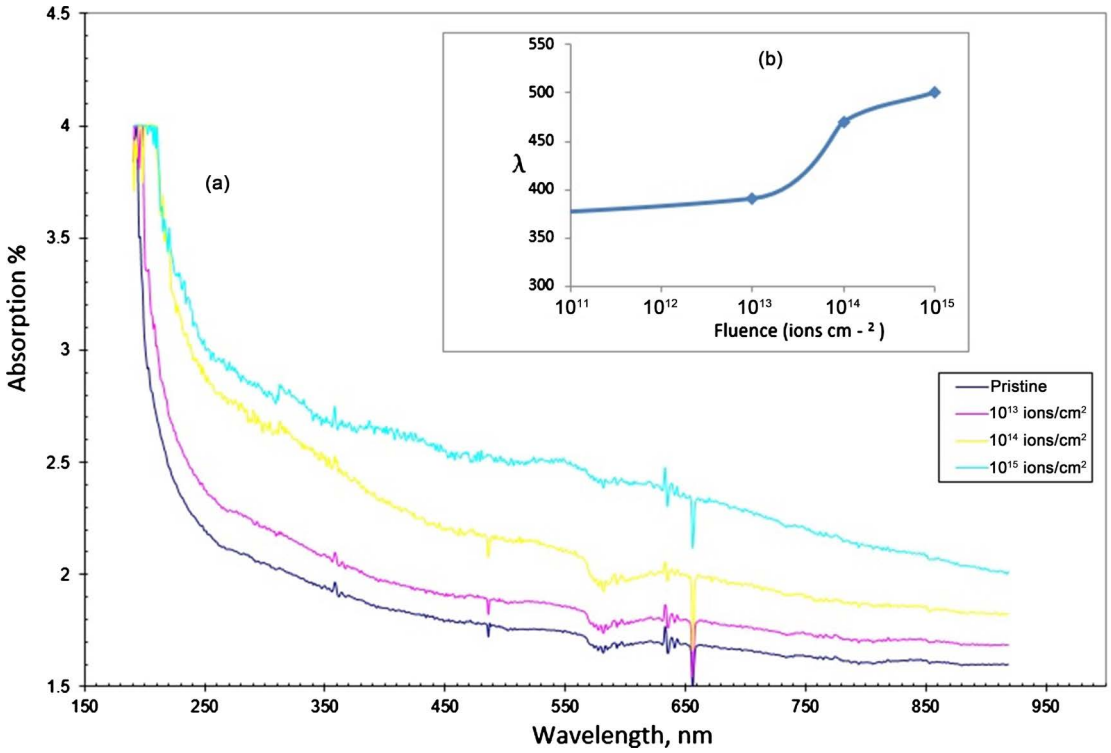

Figure 1. UV-Vis absorption spectrum for the UWMHDPE implanted by 160 keV Ar^+ ions with different influences.

greater than 10^{15} ion/cm^2. It is clear that for the sharp absorption edges in the curves of the virgin and Ar^+-implanted UHMWPE samples 656 - 662 and 482 - 492, there are no significant change in the stability of the polymers up to a influence of 10^{15} ions cm^{-2}, which shows good recyclability in the irradiation detection when a constant wavelength shifts before and after the detection of the ion beam. This sensor can be useful for the monitoring of ion bombardment and quality control in ion bombardment synthesis in the lab and biomedical industry.

The absorption coefficient $\alpha(\omega)$ of the optical absorption near the band edge shows an exponential dependence on the photon energy $\hbar\omega$ (**Figure 2(a)**), which obeys the Urbach's empirical relation (1): [24].

$$\alpha(\omega) = \alpha_0 \exp(\hbar\omega/\Delta E) \tag{1}$$

where α_0 is a constant and ΔE is the width of the band tails of the localized states.

Equation (1) can be written as:

$$\ln\alpha(\omega) = \ln\alpha_0 + \frac{\hbar\omega}{\Delta E} \tag{2}$$

The variation of the logarithmic of the absorption coefficient ($\ln\alpha(\omega)$) with the photon energy after UHMWPE exposure to irradiation is presented in **Figure 2(b)**. The experimental value for the absorption band tail energy, ΔE, of the localized state is obtained from the slope of the linear portion of curves (slope = $1/\Delta E$). **Figure 2(c)** shows the variation of ΔE with different influences.

The values of the optical energy gap for the UHMWPE before and after implantation were estimated using the Mott and Davis' model [25] for the directly and indirectly allowed transition using Equation (3):

$$\alpha(\omega)\hbar\omega = B\left(\hbar\omega - E_{opt}\right)^n \tag{3}$$

where B is a constant, α is the absorption coefficient and E_{opt} is the optical energy gap of the system and (n) is the index used to determine the nature of the electronic transitions during the absorption process. According to Equation (3), the direct and indirect transitions of $(E_{opt})^d$ and $(E_{opt})^{in}$ can be obtained by extrapolating the linear portions of the curves, which represents $(\alpha\hbar\omega)^2$ and $(\alpha\hbar\omega)^{1/2}$ compared to the photon energy ($\hbar\omega$) for UHMWPE at different ion fluences. The linear fit for this relation is shown in **Figure 3(a)** and **Figure 3(b)**. The indirect transition in many amorphous materials fit the case for $n = 2$. For direct transition, a reasonable fit of Equation (3) with $n = 1/2$ is particularly achieved at the higher absorption values found at the edge [26] [27]. The values of $(E_{opt})^d$ and $(E_{opt})^{in}$ were found to decrease slowly as the ion dose increased. A significant decrease of up to 10^{14} ion/cm^2 was followed by a gradual decrease of up to 10^{15} ion/cm^2. Such behavior is due to the crystalline structure of UHMWPE detector, which leads to the changes in the degree of disorder [28]. Davis and Mott [29] reported that the presence of high density of localized states in the band structure is responsible for the lower values of the optical gap. The variation of the optical energy gap with electronic irradiation energies and doses can be explained

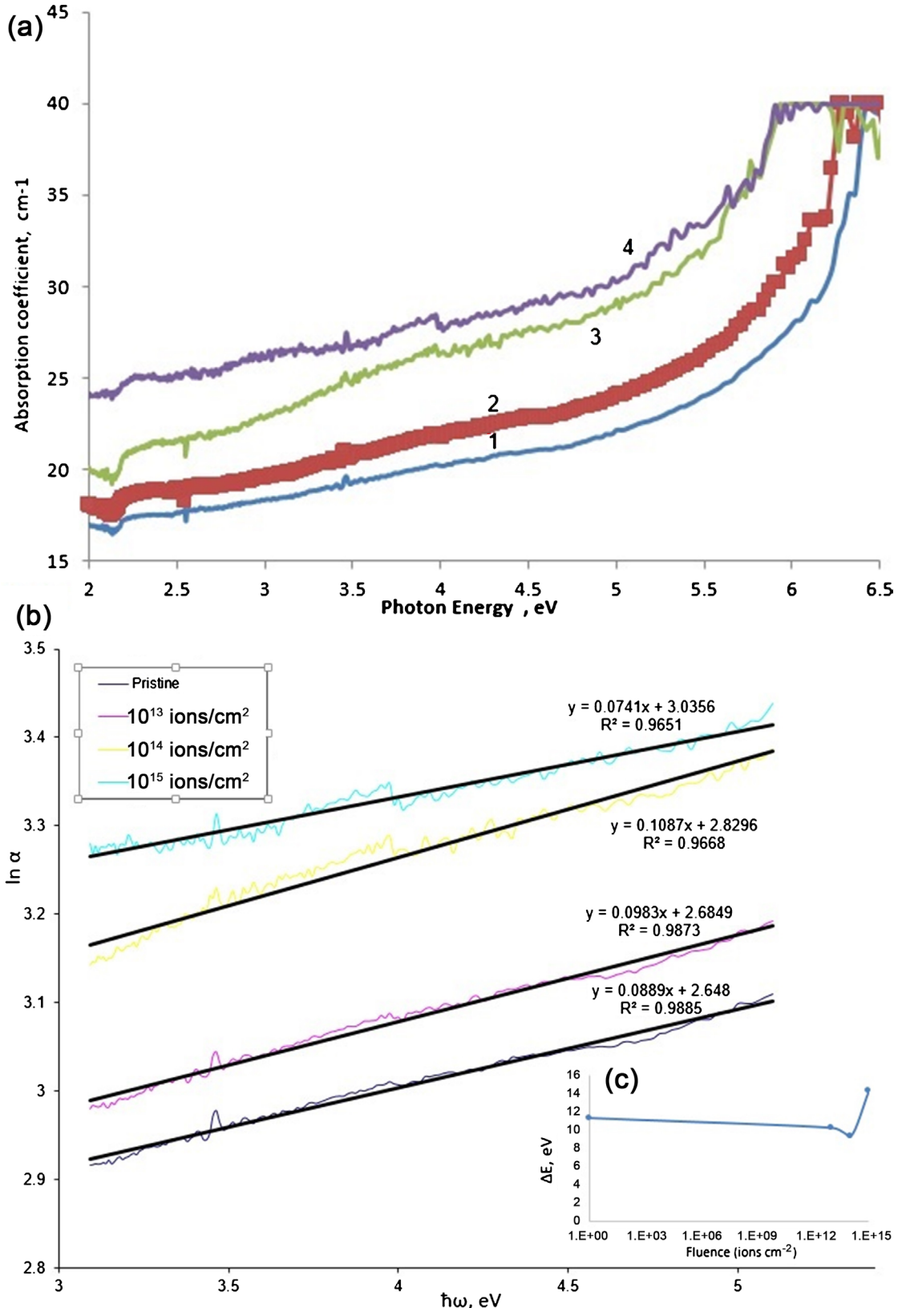

Figure 2. (a) Variation of absorption coefficient as a function of photon energy (ħω) for the UHMWPE irradiated and unirradiated samples for (1) 0; (2) 1×10^{13}; (3) 1×10^{14}; (4) 1×10^{15} ions/cm^2 influences; (b) Variation of ln α as a function of photon energy (ħω) at different influences α(ω); (c) Variation of ΔE with different influence.

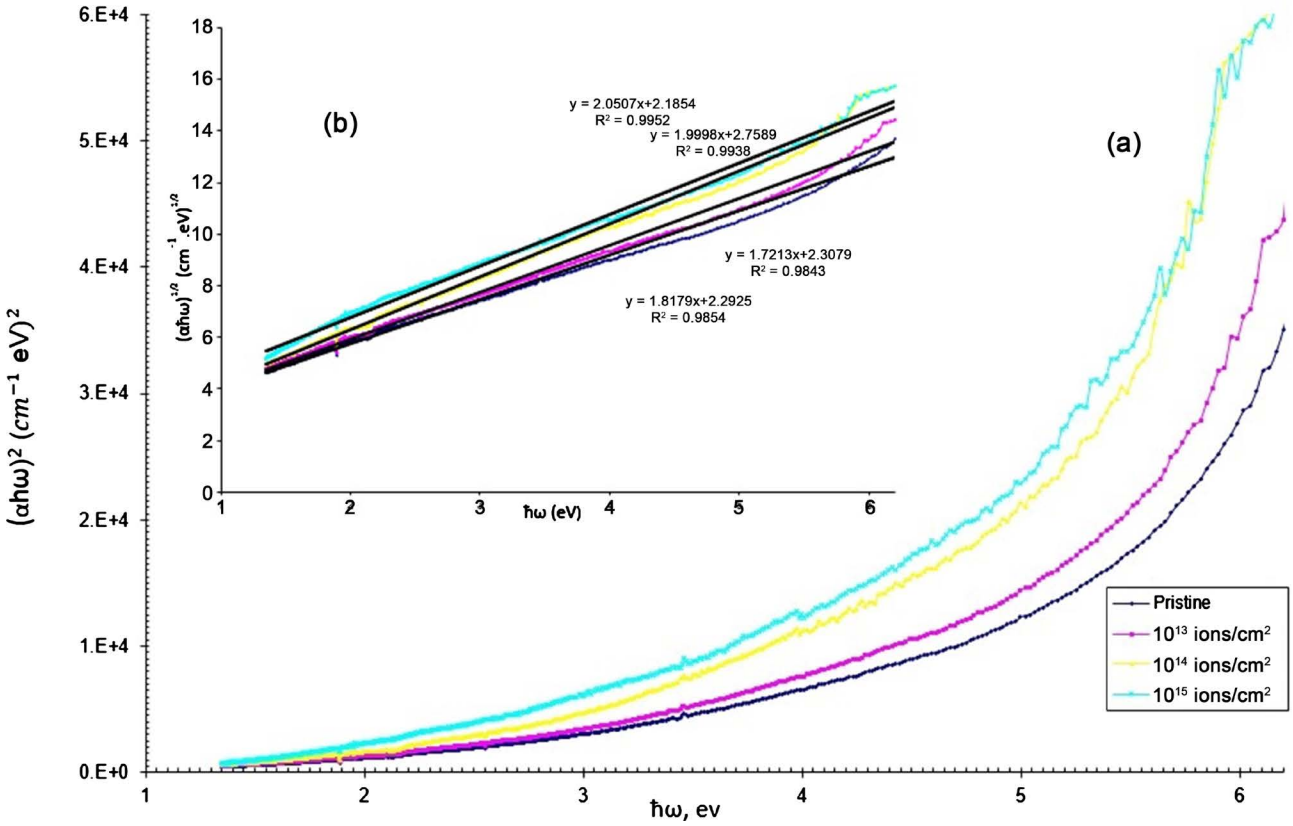

Figure 3. (a) The variation of $(a\hbar\omega)^2$ compared to ħω and (b) the linear fitting of the variation of $(a\hbar\omega)^{1/2}$ compared to $\hbar\omega$ for the non-irradiated as well as the irradiated UHMWPE with ion beams at different fluences.

as the change in the degree of disorder. From the density of state model, it is known that E_{opt} decreases with increasing degree of disorder of the amorphous phase [27]. At this stage, one may expect that a band tail can be possibly created due to irradiation. The decrease in E_{opt} leads to a shift in the band tail ΔE towards the higher energy region and hence, the values of ΔE calculated by Equation (1) are expected to increase as the radiation dose is increased. Our experimental results are consistent with theoretical consideration [30]. One should point out that the sensitivity to ion irradiation of UHMWPE detector at higher doses is appreciable. Above these higher doses, the sample suffers a crosslinking, at which the values of E_{opt} decrease slowly.

3.2. Electrical Frequency Response for UHMWPE

The implantation-induced disorder of polymers leads to a change in the conductance due to alteration of the electronic structure. Typically, the conductance increases with ion influence due to the carbonization of the polymer. An exception is the high-fluence implantation of metals, which increases the metal volume fraction and also contributes to the charge carrier transport.

Figure 4 shows the variation of electrical conductivity σ_{ac} with log frequency for the pristine and irradiated samples. A significant and exponential increase in conductivity has been observed around 300 kHz for pristine and irradiated sam-

ples. It is also observed that the variation of σ_{ac} with log frequency is identical for pristine and irradiated samples at lower frequency, while this was higher for irradiated samples at higher frequencies.

The increase in conductivity at a given frequency due to irradiation may be attributed to the scissioning of polymer chains and of the subsequent increase in the free radicals, unsaturation, etc. [31]. An ac field of sufficiently high frequency applied to a metal-polymer-metal structure may cause a net polarization, which is out of phase with the field. This results in ac conductivity and it appears at frequencies that are greater than that at which traps are filled or emptied [32]. As an example, the decrease in the resistance with an increase in the ion influences is shown in **Figure 5(b)** for the case of Ar^+-implanted UHMWPE. The graphs also demonstrate good correlation of both the direct energy band gap $(E_{opt})^d$ in **Figure 5(a)** and the decrease in resistance with the increase in ion influences.

Figure 6 shows the variation of the dielectric constant (ε) with frequency for the pristine and irradiated samples. As evident from the plot, a sharp decrease in the dielectric constant has been observed for the irradiated samples. For these samples, the dielectric constant decreases by a factor of 40 after the implantation compared to non-implantation samples. After implantation, the dielectric constant remains almost constant, except when it decreases at a sufficiently high frequency where only electronic polarization dominates. At low frequencies, the motion of the free charge carriers is constant and thus, the dielectric constant remains unchanged. As the frequency increases, the charge carriers migrating through the dielectric get trapped at defect sites and induce an opposite charge in their vicinity. Due to this, they slow down and the value of the dielectric constant decreases [33].

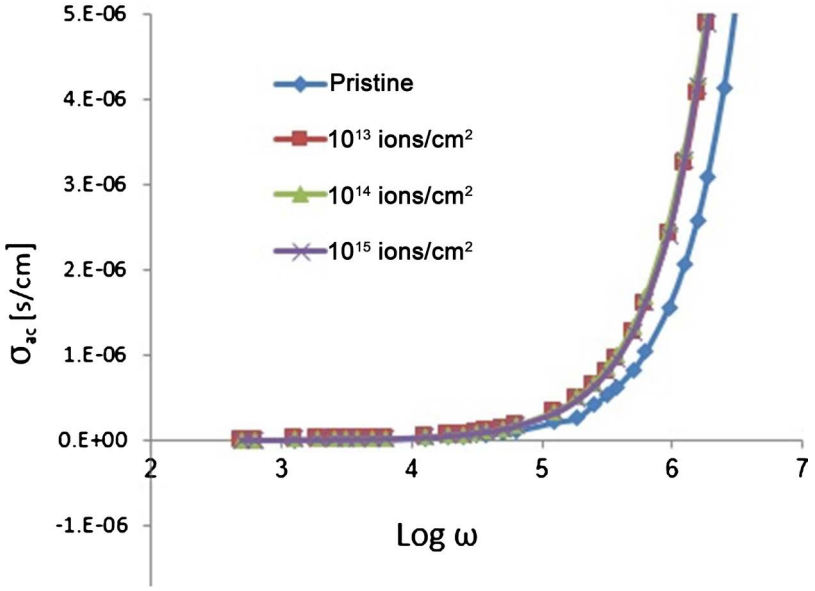

Figure 4. Plot of ac conductivity (σ_{ac}) versus log frequency for non-irradiated and irradiated UWMHDPE at different influences.

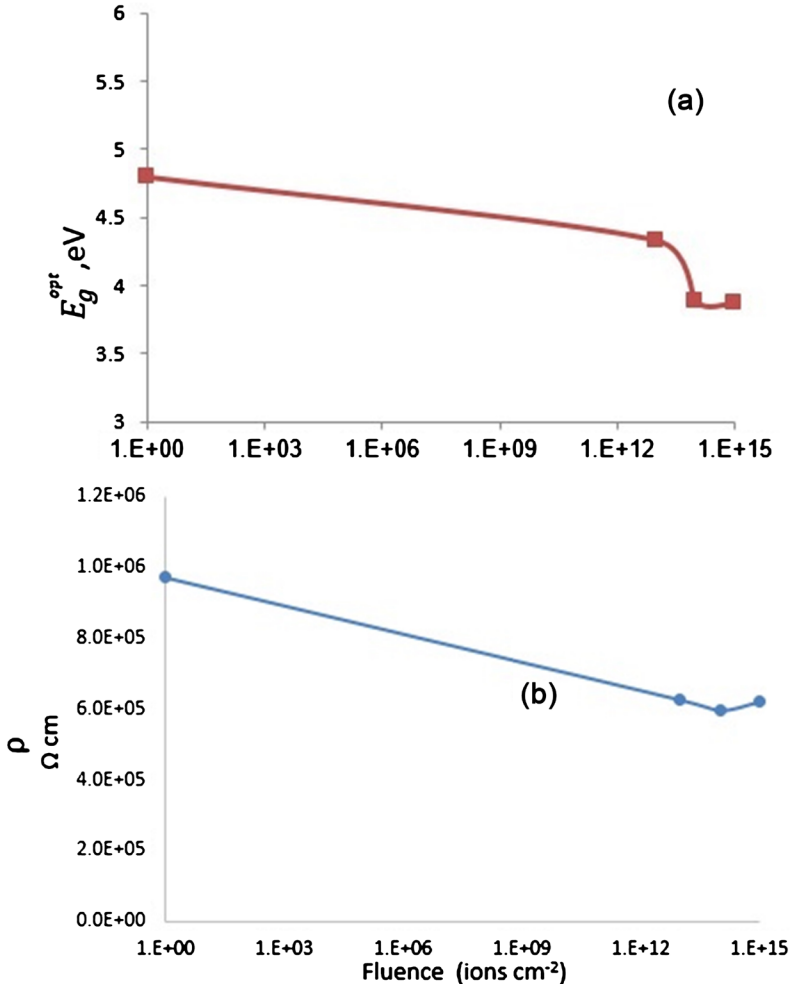

Figure 5. (a) The variation of optical band gap and (b) Resistivity versus ion influences of 160 keV argon-implanted UWMHDPE.

The plot of the dielectric loss tangents (tanδ) versus log frequency for pristine and irradiated UHMWPE samples in the frequency range of 300 Hz - 1 MHz is shown in Figure 7. It is observed that tanδ decreases with a moderate increase in frequency and no relaxation peaks are observed after the implantation. Tanδ decreases as the frequency increases and becomes negative beyond a frequency of 80 kHz for the non-irradiated and irradiated UHMWPE with ion beams up to the influence of 10^{14} ion cm^{-2}. This shows the dominance of capacitive contributions [34]. However, by increasing the dose above 10^{15} ion cm^{-2}, there is an inverse process of the reduction in tanδ, which is considerably more pronounced via degradation and crosslinking. It can be assumed that this last process is connected with the release of hydrogen during the irradiation of polyethylene, which is relatively consistent with a previous study [35].

4. Conclusion

A simple optical/ electrical sensor is demonstrated as a device to detect the ions. A study of 160 keV energy Ar^+ ion-induced effects in UHMWPE has been

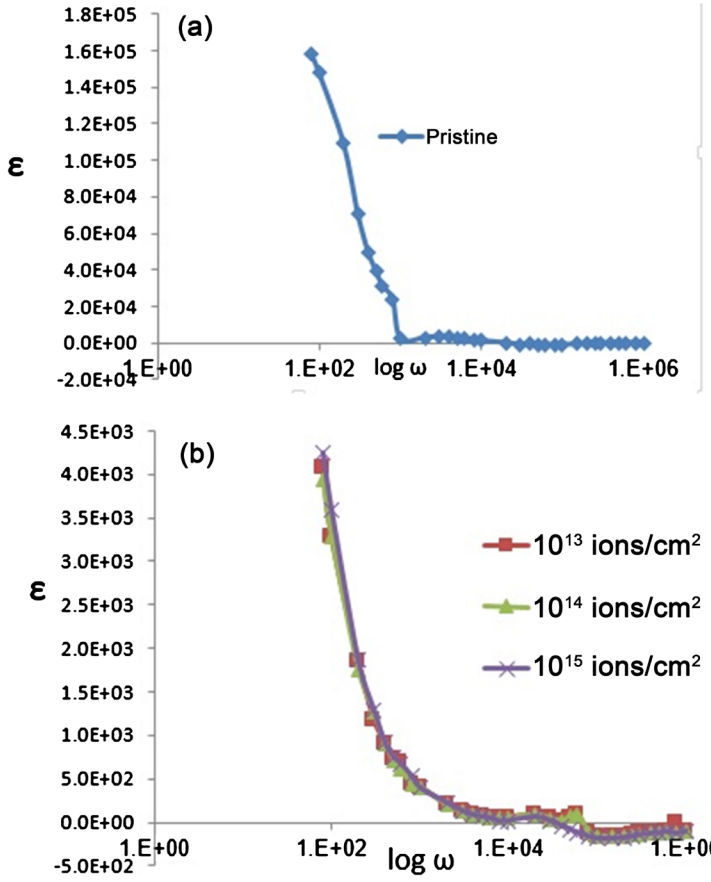

Figure 6. Plot of dielectric constant (ε) versus log frequency for (a) non-irradiated and (b) irradiated UHMWPE with ion beams at different influences.

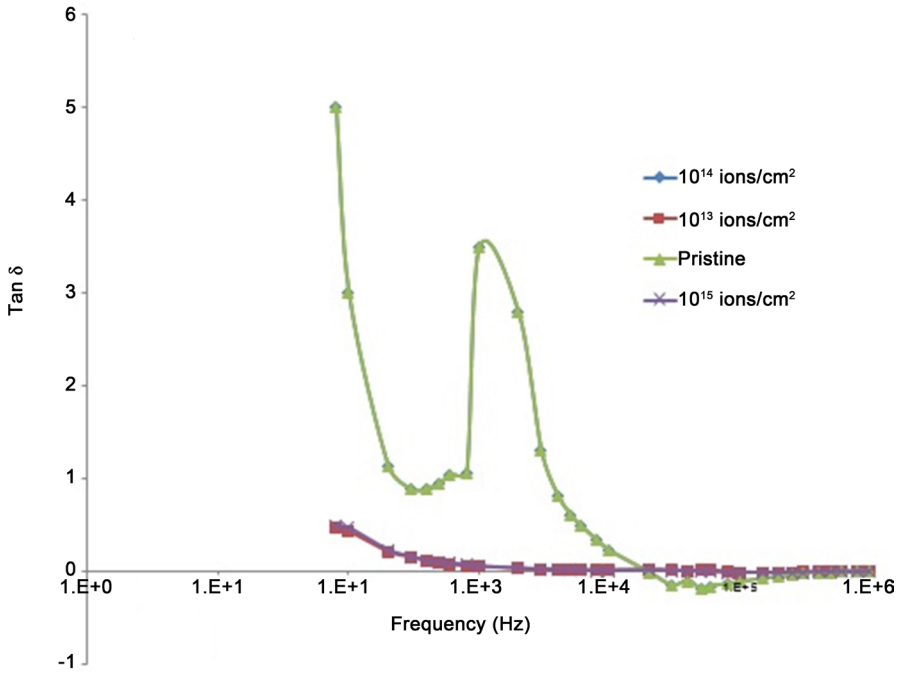

Figure 7. Dielectric loss tangent versus log frequency for pristine and Ar^+ ion beam exposed UHMWPE.

conducted. The measurements of the optical spectra in the range of 360 - 840 nm have been carried out for the unirradiated and irradiated samples and optical constants have been determined. The analysis of the results of the optical study reveals that the absorption coefficient of the polymer increases up to an influence of 10^{14} ions cm^{-2}, which is probably due to cross-linking without any degradation effects. Furthermore, these results indicate that UHMWPE gets chemically degraded at the highest Ar^+ ion influence used, which was 10^{15} ions cm^{-2}. There is an exponential increase in the conductivity with the log of frequency and the effect is significant after implantation. However, the tan δ and the dielectric constant ε decrease with an increase in ion influence. As the influence increases, the polymer surface becomes hydrogenated amorphous carbon when the influence exceeds 1×10^{15} ions/cm^2 because of the degradation of the polymer from the scissioning of bonds. This is also corroborated by optical absorption spectra of UWMHDPE implanted by 160 keV Ar^+ ions with different influences.

Conflicts of Interest

The author declares no conflict of interest.

References

[1] Lee, E.H. (1999) Ion-Beam Modification of Polymeric Materials—Fundamental Principles and Applications. *Nuclear Instruments and Methods in Physics Research Section B*, **151**, 29-41. https://doi.org/10.1016/S0168-583X(99)00129-9

[2] Dong, H. and Bell, T. (1999) State-of-the-Art Overview: Ion Beam Surface Modification of Polymers towards Improving Tribological Properties. *Surface and Coatings Technology*, **111**, 29-40. https://doi.org/10.1016/S0257-8972(98)00698-7

[3] Williams, J.S. (1986) Materials Modification with Ion Beams. *Reports on Progress in Physics*, **49**, 491-587.

[4] Ferain, E. and Legras, R. (1994) Track-Etched Membrane: Dynamics of Pore Formation. *Nuclear Instruments and Methods in Physics Research Section B*, **84**, 331-336. https://doi.org/10.1016/0168-583X(94)95725-8

[5] Kondyurin, A. and Bilek, M. (2015) Ion Beam Treatment of Polymers. Chapters 1, 2, 3 and 4. 2nd Edition, Elsevier, University of Sydney, Australia, 1-127.

[6] Spohr, R. (1990) Ion Tracks and Microtechnology: Principles and Applications. Vieweg, Brunschweig, Germany. https://doi.org/10.1007/978-3-322-83103-3

[7] El-Saftawy, A.A., Abdel Reheem, A.M., Kadil, S.A., Abd EL Aal, S.A. and Salam, S. (2016) Comparative Studies on PADC Polymeric Detector Treated by Gamma Radiation and Ar Ion Beam. *Applied Surface Science*, **371**, 596-606. https://doi.org/10.1016/j.apsusc.2016.03.044

[8] Scott, J.L., Clinard Jr., F.W. and Wiffen, F.W. (1985) Special Purpose Materials for Fusion Application. *Journal of Nuclear Materials*, **133**, 156-163. https://doi.org/10.1016/0022-3115(85)90126-6

[9] Mazzoldi, P. and Arnold, G.W., Eds. (1987) Ion Beam Modification of Insulators. Vol. 3, Chap. 8. Elsevier, Amsterdam, The Netherlands, 301-379.

[10] Koizumi, H., Ichikawa, T., Yoshida, H., Namba, H., Taguchi, M. and Kojima, T. (1996) Radical Formation in the Radiolysis of Solid Alanine by Heavy Ions. *Nuclear*

Instruments and Methods, **117**, 431-435.
https://doi.org/10.1016/0168-583X(96)00351-5

[11] Abdul-Kader, A.M., Turos, A., Jagielski, J., Nowicki, L., Ratajczak, R., Stonert, A. and Al-Madeed, M. (2005) Hydrogen Release in UHMWPE upon He-Ion Bombardment. *Vacuum*, **78**, 281-284. https://doi.org/10.1016/j.vacuum.2005.01.039

[12] Popok, V.N., Azarko, I.I., Khaibullin, R.I., Stepanov, A.L., Hnatowicz, V., Mackova, A. and Prasalovich, S.V. (2004) Radiation-Induced Change of Polyimide Properties under High-Fluence and High Ion Current Density Implantation. *Applied Physics A*, **78**, 1067-1072. https://doi.org/10.1007/s00339-003-2166-9

[13] Chen, F., Wang, X.L. and Wang, K.M. (2007) Development of Ion-Implanted Optical Waveguides in Optical Materials: A Review. *Optical Materials*, **29**, 1523-1542.
https://doi.org/10.1016/j.optmat.2006.08.001

[14] Chen, J.S., Zhu, F., Pan, H., Cao, J., Zhu, D., Xu, H., Cai, Q., Shen, J., Chen, L. and He, Z. (2000) Surface Modification of Ion Implanted Ultra High Molecular Weight Polyethylene. *Nuclear Instruments and Methods in Physics Research Section B*, **169**, 26-30. https://doi.org/10.1016/S0168-583X(00)00011-2

[15] Allen, C., Bloyce, A. and Bell, T. (1996) Sliding Wear Behaviour of Ion Implanted Ultra High Molecular Weight Polyethylene against a Surface Modified Titanium Alloy Ti-6Al-4V. *Tribology International*, **29**, 527-534.
https://doi.org/10.1016/0301-679X(95)00116-L

[16] Wu, Y., Zhang, T., Zhang, H., Zhang, X., Deng, Z. and Zhou, G. (2000) Electrical Properties of Polymer Modified by Metal Ion Impantation. *Nuclear Instruments and Methods in Physics Research Section B*, **169**, 89-93.
https://doi.org/10.1016/S0168-583X(00)00022-7

[17] Hanafy, T.A. (2008) Drastic Effects of Fast Neutrons and γ-Irradiation on the DC Conductivity of Co-, Ni-, Mn- and Ag-Gelatin Doped Films. *Current Applied Physics*, **8**, 527-534. https://doi.org/10.1016/j.cap.2007.09.002

[18] Boiteuxa, G., Chailan, J.F., Chaucharda, J. and Seytrea, G. (1997) Dielectric and Mechanical Spectroscopes for the Study of Thermal and Radiochemical Ageing of Polymers. *Nuclear Instruments and Methods in Physics Research Section B*, **131**, 172-179. https://doi.org/10.1016/S0168-583X(97)00198-5

[19] Phukan, T., Kanjilal, D., Goswami, T.D. and Das, H.L. (1999) Dielectric Response of Heavy Ion Irradiated PADC Track Detector. *Nuclear Instruments and Methods in Physics Research Section B*, **155**, 116-119.
https://doi.org/10.1016/S0168-583X(99)00255-4

[20] Durrani, S.A. and Bull, R.K. (1987) Solid State Nuclear Track Detection. Pergamon Press, Oxford, UK, 89.

[21] Turos, A., Jagielski, J., Piatkowska, A., Bielinski, D., Slusarski, L. and Madi, N.K. (2003) Ion Beam Modification of Surface Properties of Polyethylene. *Vacuum*, **70**, 201-206. https://doi.org/10.1016/S0042-207X(02)00643-7

[22] Zamani, M., Sovvides, E., Petrakis, J. and Charalambous, S. (1986) Gamma Dose Discrimination Properties of SSNT Detectors. *International Journal of Radiation Applications and Instrumentation. Part D. Nuclear Tracks and Radiation Measurements*, **12**, 141-144. https://doi.org/10.1016/1359-0189(86)90557-1

[23] Zhu, R.-Y. (1998) Radiation Damage in Scintillation Crystals. *Nuclear Instruments and Methods in Physics Research Section A*, **413**, 297-311.
https://doi.org/10.1016/S0168-9002(98)00498-7

[24] Urbach, F. (1953) The Long-Wavelength Edge of Photographic Sensitivity and of the Electronic Absorption of Solids. *Physical Review*, **92**, 1324.

https://doi.org/10.1103/PhysRev.92.1324

[25] Mott, N.F. and Davis, E.A. (1979) Electronic Process in Non-Crystalline Materials. 2nd Edition, Clarendon Press, Oxford, UK.

[26] El-Muraikhi, M. (2001) Effect of Electric Field on Optical Properties of Post Gamma-Irradiated Lithium Potassium Sulphate Crystals. *Materials Letters*, **51**, 19-26. https://doi.org/10.1016/S0167-577X(01)00258-0

[27] Kurik, M.V. (1971) Urbach Rule. *Physica Status Solidi* (*A*), **8**, 9-45. https://doi.org/10.1002/pssa.2210080102

[28] Clegg, D.W. and Collyer, A.A. (1991) Irradiation Effects on Polymers. Elsevier, London, UK; New York, NY, USA.

[29] Davis, E.A. and Mott, N.F. (1970) Conduction in Non-Crystalline Systems V. Conductivity, Optical Absorption and Photoconductivity in Amorphous Semiconductors. *The Philosophical Magazine*, **22**, 903-922. https://doi.org/10.1080/14786437008221061

[30] Sharma, P., Vashistha, M. and Jain, I.P. (2006) Optical Study of Ion-Induced Effects in $Ge_{20}Se_{80-X}Bi_X$ Thin Films. *Optical Materials*, **27**, 395-398. https://doi.org/10.1016/j.optmat.2004.09.006

[31] Popok, V.N. (2012) Ion Implantation of Polymers: Formation of Nanoparticulate Materials. *Reviews on Advanced Materials Science*, **30**, 1-26.

[32] Virk, H.S., Chandi, P.S. and Srivastava, A.K. (2001) Physical and Chemical Changes Induced by 70 MeV Carbon Ions in Polyvinylidene Difluoride (PVDE) Polymer. *Nuclear Instruments and Methods in Physics Research Section B*, **183**, 329-336. https://doi.org/10.1016/S0168-583X(01)00743-1

[33] Jonscher, A.K. (1977) The "Universal" Dielectric Response. *Nature*, **267**, 673-679. https://doi.org/10.1038/267673a0

[34] Srivastava, A.K. and Virk, H.S. (2000) 50 MeV Lithium Ion Beam Irradiation Effects in Poly Vinylidene Fluoride (PVDF) Polymer. *Bulletin of Materials Science*, **23**, 533. https://doi.org/10.1007/BF02903896

[35] Švorčík, V., Rybka, V., Stibor, I., Hnatowicz, V., Vacik, J. and Stopka, P. (1997) Synthesis of Grafted Polyethylene by Ion Beam Modification. *Polymer Degradation and Stability*, **58**, 143-147. https://doi.org/10.1016/S0141-3910(97)00038-4